III.5. Molecular Chaos: The Boltzmann Distribution

As discussed in the preceding section, multiple collisions between the particles in a gas have a ***randomizing effect*** on the directions of motion of the particles. A collision can deflect a particle either to the left or to the right, more forward or more backward, depending on the initial conditions for that collision. The ***transfer of momentum*** from projectile to the target particle, even in an elastic collision, depends crucially on the impact parameter (and the mass ratio of the colliding particles, if they are non-identical). For example, in a head-on collision of two identical particles, the target receives the full momentum of the projectile, which remains at rest after the collision. Different momentum transfers lead to different velocities $\vec{u}$ of the particles. Therefore, the particles in a gas at thermal equilibrium are characterized not by a single velocity $\vec{u}$, but by a ***probability distribution*** $f(\vec{u})$ for the velocity. It can experimentally be determined with a ***"velocity chopper"***, two co-axial gear wheels that are put into the path of the particles to be measured. The device lets only particles of a particular velocity u pass through the gaps in the wheels. The velocity can be tuned by changing the speed of revolution of the wheels.

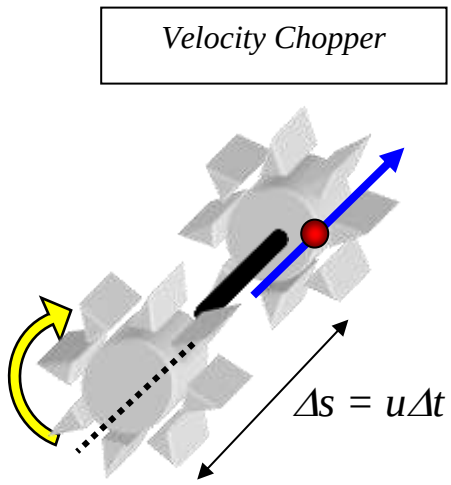

Figure III-22

The probability function $f(\vec{u})$ has a characteristic form. It represents the probability (density) ***dP*** to find within the gas a particle in the volume element $d^3\vec{u}$ at the velocity (vector) $\vec{u}$,

$$d^3P(\vec{u}) = f(\vec{u})du_x du_y du_z = f(\vec{u})d^3\vec{u} \qquad \text{(III.104)}$$

For gas particles in completely chaotic motion, no direction is preferred, and the probability $d^3P(\vec{u})$ has to be an ***uncorrelated product of the individual probabilities*** to find any of the velocity components u_x, u_y, or u_z,

$$\begin{aligned} d^3P(\vec{u}) &= dP(u_x)\cdot dP(u_y)\cdot dP(u_z) \\ &= \left[f(u_x)du_x \right] \left[f(u_y)du_y \right] \left[f(u_z)du_z \right] \end{aligned} \qquad \text{(III.105)}$$

For the same reason, the functions in the brackets must be identical functions for the three components. Furthermore, a given magnitude of a velocity component, e.g., $u_x = +500$ *m/s*, must be as likely as the same velocity in the opposite direction, i.e., $u_x = -500$ *m/s*. This implies that the function *f* in Equ. III.105 is not linear in the velocity component u_x and the other components. Similarly, the function *f* in Equ. III.104 cannot be linear in the velocity vector $\vec{u}$. The corresponding functions have to have an ***even dependence on the corresponding arguments***, for example, ***quadratic dependencies***, and one would have to write $f(u_x^2), f(u_y^2), f(u_z^2), f(\vec{u}^2)$, respectively. (Rigorously, one should use a different name for this type of function, e.g., $g(u^2) = f(\vec{u})$ instead of simply renaming $f_{new}(u^2) = f_{old}(\vec{u})$). In any case, because of Equs. III.104 and 105, one has to require that the new function *f* behaves like

$$f(u^2 = u_x^2 + u_y^2 + u_z^2) = f(u_x^2)\cdot f(u_y^2)\cdot f(u_z^2) \qquad \text{(III.106)}$$

The relation III.106 indicates a peculiar dependence of the probability density *f* on its variables. In fact, apart from the trivial and unrealistic function $f\left(u_i^2\right) = const.$, there is only one non-trivial

mathematical function that shows this behavior: $f\left(\vec{u}^2\right)$ and all $f\left(u_i^2\right)$ (i = x,y,z) have to be exponentials in the u^2 variables, for example,

$$f(u^2)=C\cdot e^{-au^2} \qquad \text{(III.107)}$$

where a and C are constants yet to be determined. The ***constant a has to be a positive number***, a negative number would make the probability become indefinitely large for large velocities, which makes physically no sense. If $f\left(\vec{u}^2\right)$ is supposed to be a probability (more accurately: probability density), it ***must be normalizable***, the sum (integral) of all probabilities has to equal unity:

$$1=\int_{-\infty}^{+\infty} du\, f(u^2)=C\cdot\int_{-\infty}^{+\infty} du\, e^{-au^2} \qquad \text{(III.108)}$$

This condition determines the normalization constant to $C = \sqrt{(a/\pi)}$. The constant a can also be determined, since the average squared velocity is already known from Equ. III.79:

$$\begin{aligned}\bar{\varepsilon}_x &= \frac{m}{2}\overline{u_x^2}=\frac{m}{2}\int_{-\infty}^{+\infty} du_x\cdot f\left(u_x^2\right)u_x^2 \\ &= \frac{m}{2}\sqrt{\frac{a}{\pi}}\cdot\int_{-\infty}^{+\infty} du_x\cdot u_x^2\cdot e^{-au_x^2}\end{aligned} \qquad \text{(III.109)}$$

The integrand in III.109 is an ***even function of u_x*** and, hence, the value of the integral is twice that taken only along the positive ***u_x***-axis:

$$\int_{-\infty}^{+\infty} du_x\, u_x^2\, e^{-a u_x^2} = 2 \cdot \int_{0}^{+\infty} du_x\, u_x^2\, e^{-a u_x^2} = \frac{1}{2a}\sqrt{\frac{\pi}{a}} \qquad \text{(III.110)}$$

Combining Equs. III.109 and 110, one obtains

$$\bar{\varepsilon}_x = \frac{1}{2} k_B T = \frac{m}{2}\sqrt{\frac{a}{\pi}} \cdot \frac{1}{2a}\sqrt{\frac{\pi}{a}} = \frac{m}{4a} \qquad \text{(III.111)}$$

This determines the unknown parameter ***a = m/(2k$_B$T)***, yielding an overall velocity distribution of the gas particles of

$$f(u_x) = C \cdot e^{-a u_x^2} = \sqrt{\frac{m}{2\pi k_B T}} \cdot exp\left\{-\frac{m u_x^2}{2 k_B T}\right\} \qquad \text{(III.112)}$$

for one (the *x*-) velocity component. Then, using Equ. III.106, the probability distribution for the total velocity is obtained from Equ. III.112 by multiplying three equal terms of the same form, such that

$$f(\vec{u}) = g(\vec{u}^2) = \left(\frac{m}{2\pi k_B T}\right)^{3/2} \cdot exp\left\{-\frac{m u^2}{2 k_B T}\right\} \propto exp\left\{-\frac{\varepsilon(\vec{u})}{k_B T}\right\} \qquad \text{(III.113)}$$

This is the famous ***Maxwell-Boltzmann velocity distribution,*** also termed ***"statistical"*** spectrum. Note that ***the probability to find a given velocity (vector) depends on the Boltzmann factor, the exponential of the negative ratio of the energy associated with the observable in question and the characteristic thermal energy package k$_B$T***. This is an example of a general principle discussed in more detail in the context of partition functions.

More precisely, Equ. III.113 is a ***probability density***:

$$f(u_x)=\frac{dP(u_x)}{du_x} \qquad \text{(III.114a)}$$

and similar for the other components, such that for the velocity vector,

$$f(\vec{u})=\frac{d^3P(\vec{u})}{d^3\vec{u}} \qquad \text{(III.114b)}$$

In order to obtain a dimensionless, normalized probability ΔP, one has to multiply f(u$_x$) by a velocity difference Δu$_x$ or $f(\vec{u})$ ***by the 3D-volume element*** $d^3\vec{u}$ **.**

As an example of the use of the velocity distribution, one may calculate the average *x*-velocity component u_x of the particles (mass *m*) in a gas at temperature *T*. From Equ. III.112, one obtains

$$\langle u_x\rangle=\sqrt{\frac{m}{2\pi k_BT}}\int_{-\infty}^{+\infty}du'_xu'_x\cdot exp\left\{-\frac{mu'^2_x}{2k_BT}\right\}=0 \qquad \text{(III.115a)}$$

This follows, because the integrand is an ***odd function of u$_x$'***, hence, the negative contributions are canceled by the positive ones. Physically, this result means that neither the positive nor the negative *x* direction is preferred, as should be the case for truly random motion. On the other hand, the average ***speed in x-direction is obviously non-zero,*** $|u_x|\ \gamma\ 0$, mathematically because

$$\langle|u_x|\rangle=\sqrt{\frac{m}{2\pi k_BT}}\int_{-\infty}^{+\infty}du'_x|u'_x|\cdot exp\left\{-\frac{mu'^2_x}{2k_BT}\right\}=$$

$$=2\sqrt{\frac{m}{2\pi k_BT}}\int_{0}^{+\infty}du'_xu'_x\cdot exp\left\{-\frac{mu'^2_x}{2k_BT}\right\} \qquad \text{(III.115b)}$$

With a variable transformation $v = u_x$'$\exists\sqrt{(m/2k_BT)}$, one obtains an integral solved in any of the familiar integral tables:

$$\langle|u_x|\rangle = \frac{2}{\sqrt{\pi}}\sqrt{\frac{2k_BT}{m}}\int_0^\infty dv\cdot v\cdot exp\{-v^2\} = \sqrt{\frac{2k_BT}{m}} \qquad \text{(III.115c)}$$

Similarly, one can calculate the average of u^2, the ***mean-square velocity*** $©u^{2}™$. Because of Equ. III.115a, this velocity is equal to the variance $\sigma^2_{u_x}$ ***in the velocity distribution for the x direction***

$$\sigma^2_{u_x} = \langle u_x^2\rangle - \langle u_x\rangle^2 = \frac{2}{\sqrt{\pi}}\frac{2k_BT}{m}\int_0^\infty dv\cdot v^2\cdot exp\{-v^2\} = \frac{k_BT}{m} \qquad \text{(III.116)}$$

which is related to Equs. III.76 and 77, the average kinetic energy for motion along the *x*-degree of freedom. Note that $©|u|^{2}™ \gamma ©u^{2}™$. Hence, the velocity distribution of Equ. III.113 is a Gaussian with a variance equal to the quantity $k_BT/m = 2\,©\varepsilon_x™$, i.e., ***fluctuations in the velocity are determined by the average kinetic energy***.

As an illustration, Fig. III-23 depicts the normalized Maxwell-Boltzmann velocity distributions (velocity variable *v*) for O_2 at temperatures of *T = 1000K (solid, red)* and *T= 2000K (dots, blue)*, as calculated with the simple MATHCAD program MATHCAD_252\Maxw_Boltzm_VE.mcd. Actually plotted is the differential probability

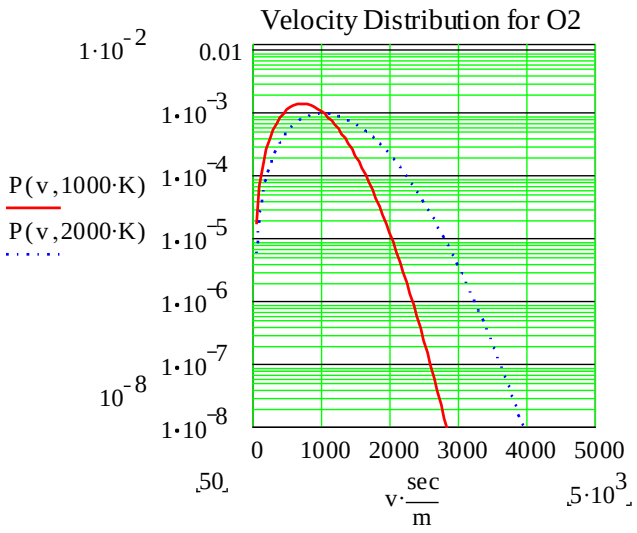

Figu

$$\frac{dP(v)}{dv} = 4\pi v^2 \cdot f(\vec{v}),$$

whose significance will be explained further below. The differential probabilities have magnitudes of the order of $10^{-3}/(m/sec)$. Since typical velocities range up to several $10^3 m/sec$, such probabilities are reasonable.

As exemplified by Fig. III.23, thermal velocity spectra have an asymmetric bell shape with a maximum at relatively low velocities. This maximum indicates the ***most probable velocity*** for the gas particles. Towards high velocities, the spectra decay rapidly, with a Gaussian character (not a log straight line, but a curve). Although there is a non-zero probability to find velocities several times as high as the most probable velocity, the probability for such high velocities is exceedingly small. As the temperature is increased, the spectra become broader, and the most probable velocity shifts to higher values.

The Maxwell-Boltzmann velocity (better: speed) distribution of Equ. III.113 contains information only on the probability to find a given speed but has lost information on the ***angular dependence of the probability***. In the case of random motion in space, of course, this dependence is trivial, since there is no preferred direction. The probability to find particles of a given speed in a given angular range with respect to some coordinate system is independent on the angles. One says: The angular ***velocity distribution is isotropic***.

Angular dependencies are best expressed in terms of spherical coordinates, ***{u, θ, ϕ}***. In such a coordinate system, the volume element is expressed as

$$d^3\vec{u} = du_x du_y du_z = u^2 du\, d\Omega = u^2 du\, d\phi\, d\theta \sin\theta \quad \text{(III.117)}$$

Because of its isotropy, the probability to find a particle at ***speed (u>0 !)*** in the range [*u*, *u*+*du*] traveling in the direction defined by polar and azimuth angular intervals { $\boldsymbol{\Omega}, \boldsymbol{\Omega}+\boldsymbol{d\Omega}$}={$\theta,\theta+d\theta$; ϕ, $\phi+d\phi$},

$$\frac{dP(u,\theta,\phi)}{u^2 du d\Omega} = f(\vec{u}) = \left(\frac{m}{2\pi k_B T}\right)^{3/2} \cdot \exp\left\{-\frac{mu^2}{2k_B T}\right\} \quad \text{(III.118)}$$

does not depend on these angles, which do not appear on the *r.h.s.* of Equ. III.118. Consequently, the probability to find a speed $u = |u|$ is simply obtained from Equ. III.118 by integration over all angles:

$$\frac{dP(u)}{du} = 4\pi\left(\frac{m}{2\pi k_B T}\right)^{3/2} \cdot u^2 \cdot exp\left\{-\frac{mu^2}{2k_B T}\right\} \quad \text{(III.118a)}$$

This is the form of the probability to be used when angle-integrated quantities associated with speed or velocity are to be computed. For example, the average speed $|u|$ should be calculated using the probability of Equ. III.118a, while the average speed $|u_x|$ for one component, e.g., the one in *x* direction, should be calculated from Equ.III.112, which does not contain a u^2-factor. This latter procedure has been carried out in Equ. III.115c.

It is then possible to calculate the characteristic speeds and velocities of interest to the random molecular scattering process occurring in a gas. For example, the average speed of a particle in a gas is given by

$$\langle |u| \rangle = \int_0^\infty du\, u \cdot \frac{dP(u)}{du} = 4\pi \left(\frac{m}{2\pi k_B T} \right)^{3/2} \int_0^\infty du\, u^3 \cdot exp\left\{ -\frac{mu^2}{2k_B T} \right\} =$$

$$= 4\pi \left(\frac{m}{2\pi k_B T} \right)^{3/2} \cdot \frac{1}{2} \left(\frac{2k_B T}{m} \right)^2 = \sqrt{\frac{8k_B T}{\pi m}} \qquad \text{(III.119)}$$

The mean-square velocity is calculated analogously.

It is slightly more involved to calculate the average relative speed, because it involves two particles, ***1*** and ***2***, simultaneously. These particles have masses m_1 and m_2 and velocities $\vec{u}_1$ and $\vec{u}_2$. As discussed previously, the ***relative velocity*** is equal to the difference $\vec{u}_{12} = \vec{u}_1 - \vec{u}_2$. The other relevant velocity vector is the velocity $\vec{u}_{cm}$ of the center of mass in the laboratory system. That is, one considers the transformation of variables

$$\left.\begin{matrix} \vec{u}_1 \\ \vec{u}_2 \end{matrix}\right\} \Leftrightarrow \begin{cases} \vec{u}_{12} = \vec{u}_1 - \vec{u}_2 \\ \vec{u}_{cm} = \dfrac{1}{m_1 + m_2} \left(m_1 \vec{u}_1 + m_2 \vec{u}_2 \right) \end{cases} \qquad \text{(III.120)}$$

Both left and right set of velocities in Equ. III.120 represent the same number of independent degrees of freedom describing the velocity vectors of the two particles completely and equivalently. One can picture the motion of the two original particles also in terms of the two hypothetical particles: one with the reduced mass

$\mu = m_1 \cdot m_2 / (m_1 + m_2)$ moving with the relative velocity $\vec{u}_{12}$ and a heavy particle, representing the center of mass of the two-particle system, with a mass $M = m_1 + m_2$ and moving with the velocity $\vec{u}_{cm}$. The arguments made earlier for the functional form of the velocity distributions for different degrees of freedom can be generalized to these two hypothetical particles. Therefore, both hypothetical particles have velocity distributions of the type of Equs. III.118, 118a, except for the different masses. Consequently, the average relative speed of two particles of arbitrary masses in a gas at equilibrium temperature T is given by the generalized formula of Equ. III.119:

$$\langle |\vec{u}_{12}| \rangle = \langle u_{12} \rangle = \sqrt{\frac{8 k_B T}{\pi \mu}} \qquad \text{(III.121)}$$

Comparison with Equ. III.119 for equal particles shows that

$$\langle |\vec{u}_{12}| \rangle = \sqrt{2} \langle |\vec{u}_1| \rangle \qquad \text{(III.122)}$$

a relation invoked already previously (cf. Equ. III.93b). This is the speed that should be used in calculations of collision frequencies among equal or different particles of a gas.

It is also straight-forward to derive the associated Maxwell-Boltzmann energy distribution, by transforming Equ. III.118 to particle ***kinetic energy*** $\varepsilon = (m/2)u^2$. One notices that the probability $dP(\vec{u})$ to find particles with velocities between u and $u+du$ in the solid-angle element $d\Omega$ is the same as that, $dP(\varepsilon)$, for particles of the ***corresponding energies*** between $\varepsilon = (m/2)u^2$ and $\varepsilon + d\varepsilon$ in the same

element $d\Omega$. Since $d\varepsilon = mu\exists du$ and $u^2du=(u/m)\, d\varepsilon$, and using the ***chain rule of differentiation***, one has

$$\frac{dP(\vec{u})}{u^2 du d\Omega} = \frac{d^2P(\varepsilon)}{u^2 d\varepsilon d\Omega}\frac{d\varepsilon}{du} = \frac{d^2P(\varepsilon)}{d\varepsilon d\Omega}\frac{m}{u} \qquad \text{(III.123)}$$

From this equation and Equs. III.111-118, one obtains the differential

Maxwell-Boltzmann kinetic-energy spectrum

$$\frac{dP(\varepsilon)}{d\varepsilon d\Omega} = \frac{u}{m}\frac{dP(\vec{u})}{d^3\vec{u}} = \sqrt{2}\left(\frac{1}{2\pi k_B T}\right)^{3/2} \cdot \sqrt{\varepsilon}\cdot e^{-\frac{\varepsilon}{k_B T}} \qquad \text{(III.124)}$$

Note that this spectrum does not depend on the particle species at all! It is the same for particles of any mass. Because there is no angle dependence of the energy spectrum, the angle-integrated spectrum is equal to that of Equ. III.124, just scaled up by a factor of 4π, since $\int d\Omega = 4\pi$ is the total solid angle (see tutorial),

$$\frac{dP(\varepsilon)}{d\varepsilon} = 4\pi\frac{u}{m}\frac{dP(\vec{u})}{d^3\vec{u}} = \frac{2\pi}{(\pi k_B T)^{3/2}}\sqrt{\varepsilon}\cdot e^{-\frac{\varepsilon}{k_B T}} \qquad \text{(III.125)}$$

The figure below illustrates, on a logarithmic scale, the shape of ***Maxwell-Boltzmann*** energy distributions for *generic* particles in a gas at the two very different temperatures of $T = 300K$ and $T = 1000K$ (MATHCAD_252\Maxw_Boltzm_VE.mcd).

Plotted are the probabilities for finding in the gas a molecule with an energy of ε. ***Typical energies are of the order of 10^{-19} J***. The approximately exponential character of the velocity distribution is clearly visible on the logarithmic scale. Except for the square-root ($\sqrt{\varepsilon}$) dependence at low energies, the distributions have an exponential character reflecting the temperature,

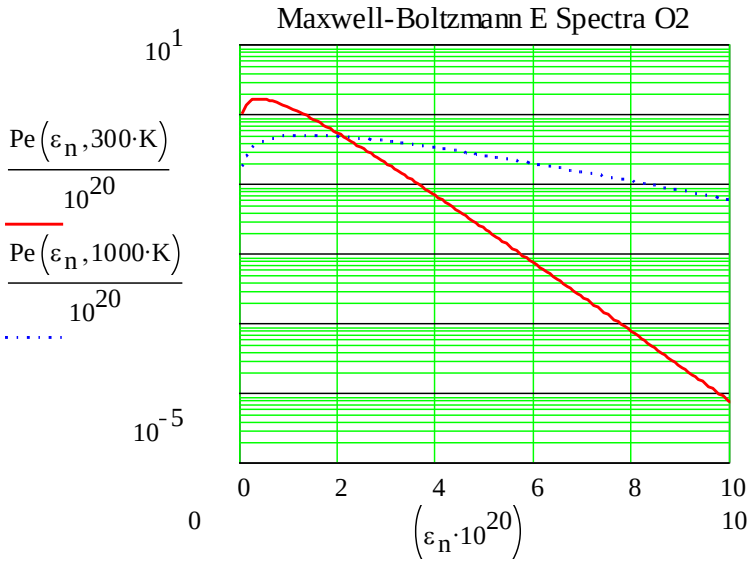

$$\lim_{\varepsilon\to\infty}\frac{d}{d\varepsilon}\ell n\frac{dP(\varepsilon)}{d\varepsilon}\approx-\frac{1}{k_BT} \qquad \text{(III.126)}$$

This suggests a simple an***d elegant method to measure the temperature*** of a gas. Clearly, the $T = 1000\ K$ spectrum is much harder ("*shallower*") than that for the lower temperature, demonstrating the important fact that ***the logarithmic slope of the energy spectrum is a direct measure of the temperature of the gas***. However, caution should be exercised in practical cases, where the limit of $\varepsilon \to \infty$ cannot be taken, because the spectra contain no significant intensity at high energies.

The single-particle kinetic energies are typically only of the order of 10^{-19} *J*. When plotted in units of J^{-1}, the probabilities have extremely small magnitudes. Hence, one often quotes kinetic energies

and related variables for moles of particles ($N = 6.10^{23}$ particles). For an N-particle system, one has to multiply the expressions (e.g., Equs. III.124 and 125) with N, in order to find the number of particles at a given energy.

The ***analytical*** Maxwell-Boltzmann ***formulas*** (Equs. III.108-111) derived above suggest a smooth behavior of the associated probabilities. However, a ***finite number of particles can obviously not have a smooth behavior,*** as far as their actual velocity and energy distributions are concerned, which show ***statistical fluctuations*** about the general shapes predicted by theory. A way of illustrating such statistical distribution is by ***sampling*** these formulas by Monte Carlo methods.

The results of such a simulation are shown in the Fig. III-25 representing "snapshots" of the kinetic-energy distributions for ideal gases of *1000* particles at *T=300K* (left) and at *T=500K* (right) (MATHCAD_252\Boltzmann_MonteCarlo.mcd), illustrating ***microstates of the system***. Here the kinetic energies of the particles are given in multiples of the Boltzmann constant k_B, i.e., as ε/k_B. These ratios have units of *K(Kelvin)* represent temperatures. The number n simply numbers the gas particles.

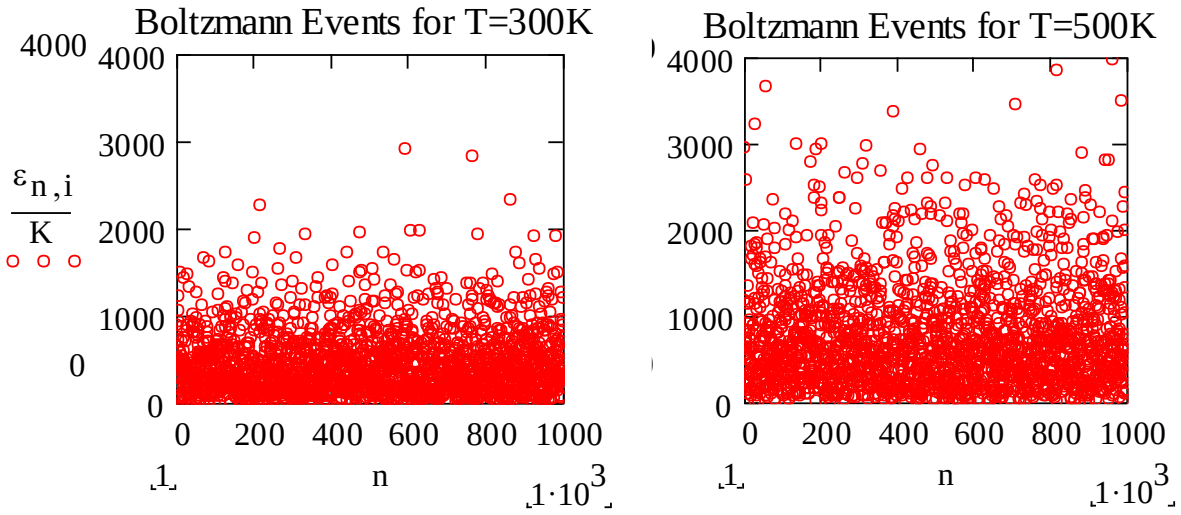

Figure III-25: Maxwell-Boltzmann energy distributions

From Fig. III.25 above, one observes that the particles are more concentrated at lower energies, near the bottom of the "scatter plot". Towards higher energies, the density of particles decreases exponentially, on average it is given by Equ. III.125. Nevertheless, there are a few particles present in the spectrum with very high energies. For the higher temperature (*T=500K*) shown in Fig. III.25 on the right, the distribution of particle energies is broader and somewhat less dense, and the density changes less rapidly with energy, than at *T=300K*.

Because of the continuous scattering and re-scattering of the particle, the distributions of all variables change dynamically in time, they fluctuate about the thermodynamic average. This effect is illustrated in an animation (***click on to view***) showing the time-dependent fluctuations in this energy distribution for *T = 300K*. For this temperature, the figure below (Fig. III-26) illustrates how the two first moments ***of the distribution*** in energies, average energy (©ε^{TM} = εaver) and the variance (σ_ε^2 = εvar) of the particle kinetic energies change with time, proceeding here with snapshot number *i*. Note that

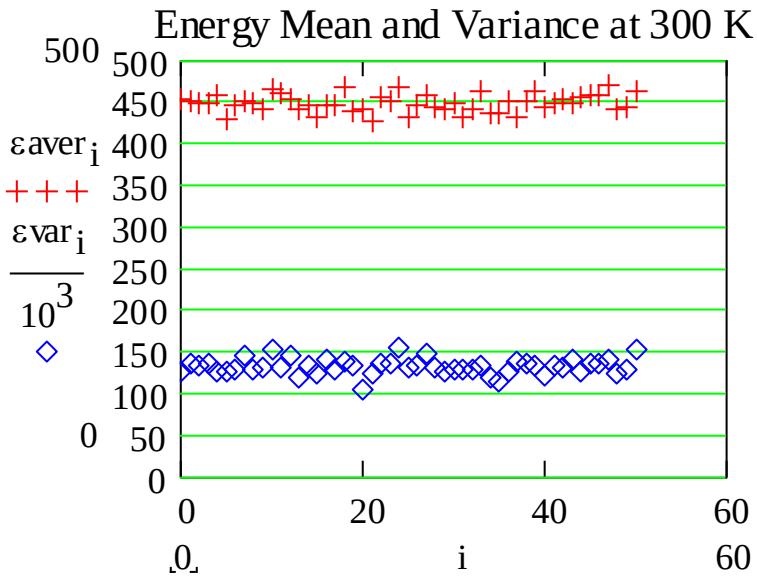

Figure III-26:Average and variance of a Maxwell-Boltzmann distribution

the ordinate scale is double-valued, the units are *K* for the average energy and K^2 for the variance.

In analogy to the earlier discussion of the average and variance (*1st* and *2nd* moment) of the velocity distribution, the average kinetic energy and its spread are defined in terms of the distribution function of Equ. III.125. For example, the average kinetic energy is given by

$$\langle \varepsilon \rangle = \int_0^\infty d\varepsilon \cdot \varepsilon \cdot \frac{dP(\varepsilon)}{d\varepsilon} = \frac{2\pi}{(\pi k_B T)^{3/2}} \int_0^\infty d\varepsilon \varepsilon^{3/2} e^{-\varepsilon/k_B T} \qquad \text{(III.127)}$$

and

$$\langle\varepsilon\rangle = \frac{2\pi}{(\pi k_B T)^{3/2}} 2\int_0^\infty d(\sqrt{\varepsilon})\sqrt{\varepsilon}^4 e^{-\sqrt{\varepsilon}^2/k_B T} = \tag{III.127a}$$

$$= \frac{4\pi}{(\pi k_B T)^{3/2}} \frac{3}{2^3 (1/k_B T)^2} \sqrt{\pi k_B T} = \frac{3}{2} k_B T$$

in agreement with earlier conclusions (Equ. III.76) based on a comparison of the phenomenological *EOS* and a microscopic evaluation of the pressure of an ideal gas. In the evaluation of the integral in Equ. III.127a, use is made of a variable transformation $x := \sqrt{\varepsilon}$.

In the case illustrated in the figures above, the average is of the order of $450\,K$, in agreement with the expectations based on Equs. III.127. The variance is of the order of $1.3 \exists 10^5\,K^2$. The square-root of the variance, the standard deviation σ_ε, is therefore of the same order as the average, which is the sign of an intrinsically broad distribution. One observes that, as time proceeds (*i* increases), the fluctuations (σ_ε^2) grow and subside again. This implies that, from time to time, some particles can accumulate a substantial amount of energy, while the rest has relatively little energy per particle. It is an interesting project to study the dependence of these fluctuations on the number *N* of particles in the gas. It is plausible to expect ***large thermal fluctuations for small systems***, as compared to a system with more particles with the ***same total energy***.

Such ***thermal fluctuations are very important*** for an understanding of spontaneous, sudden, and sometimes dramatic changes in otherwise smooth evolution processes occurring in nature. Reactions between particles and systems, spontaneous mutation and decay processes are examples where fluctuations are important. For instance, the above energy fluctuations allow particles to escape a

confining field, even though the average kinetic energy per particle would not be sufficient for such an escape

Consider a gas placed in an ***external field U(h)***, for example in the gravitational field of the Earth, in the electric field of a semiconductor (for charged particles such as electrons), or in a chemical potential. The particles can move along the "altitude" coordinate *h*, against the repulsive action of an increasing potential energy, in accordance with what their kinetic energy allows. It is clear that only those particles are found at positions $h \mu h_0$, whose kinetic energies were originally larger than the potential at h_0, i.e., $\varepsilon \mu U(h_0)$.

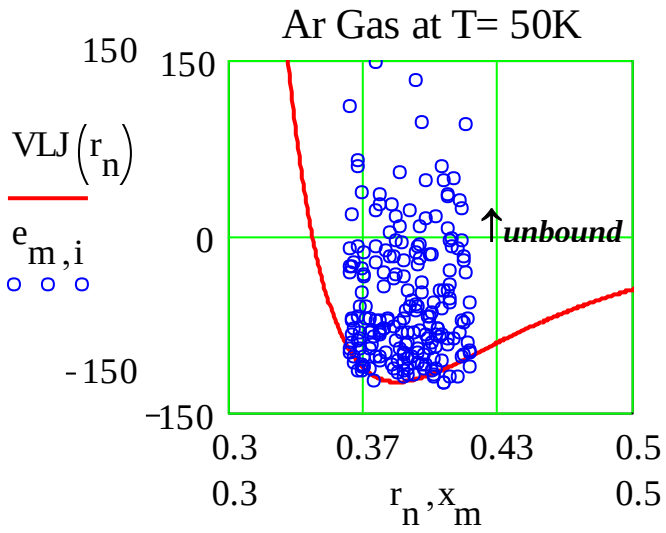

Figure III- 27: Particles in a LJ potential

Therefore, Figs. III.26 may also be taken to illustrate the density distribution of gas particles in the atmosphere or of electrons in the electric field of a semiconductor. For similar reasons, the kinetic-energy distributions determine the rates of chemical reactions. If there is a ***retaining potential barrier*** of height *B*, only particles with $\varepsilon \mu B$ can escape from the potential and take part in a reaction. As an example, Fig. III.27, drawn to scale, illustrates the distribution in kinetic energies of *Ar* particles in a gas at a relatively low temperature of *T = 50K*, relative to the interaction potential already discussed. Particles with total energies, kinetic plus potential energies,

$$\varepsilon + V \mu 0 \qquad \text{(III.128)}$$

can escape the range of the attractive van der Waals (here, Lennard-Jones) force (see also the animation). Particles with $\varepsilon + V < 0$ remain bound by the potential. In the above case, as gathered from the figure, most of the particles remain tightly bound, probably in a dense liquid or even in an ordered crystal lattice. Only relatively few particles, those belonging to the exponential, high-energy tail in the kinetic-energy distributions, have positive total energies and may move around relatively freely within the volume (are ***boiled off the condensed-phase substance***). Almost all particles are expected to feel the effect of the interaction, and the situation is far removed from that of an ideal gas.

In general, because of the exponential character of the kinetic-energy distributions, reaction rates increase exponentially with the temperature of the particles.

So far, only the velocity, energy, and angular distributions of the particles in a gas of structureless, non-interacting particles in random motion have been discussed. The ***spatial coordinates*** $\vec{r}_i = \{x_i, y_i, z_i\}$ of the particles have not been invoked at all. However, the spatial dependence of the total distribution function is trivially uniform, $dP(\vec{r}) \propto d^3\vec{r}$. This is naively expected, because there is no space-fixed retaining field, except for the container walls of the system limiting its overall size. However, the additional tacit assumption is made that there are ***no self-organizing effects*** of the system, either, that could lead to the appearance of non-uniform spatial structure. To the extent that there are no significant interactions in the ideal gas, this assumption must be valid.

Requiring normalization of the probability, one then has a random differential probability distribution of the form

$$\frac{dP(\varepsilon,\vec{r})}{d\varepsilon d^3\vec{r}} = \frac{1}{V}\cdot\frac{dP(\varepsilon)}{d\varepsilon} \qquad \text{(III.129)}$$

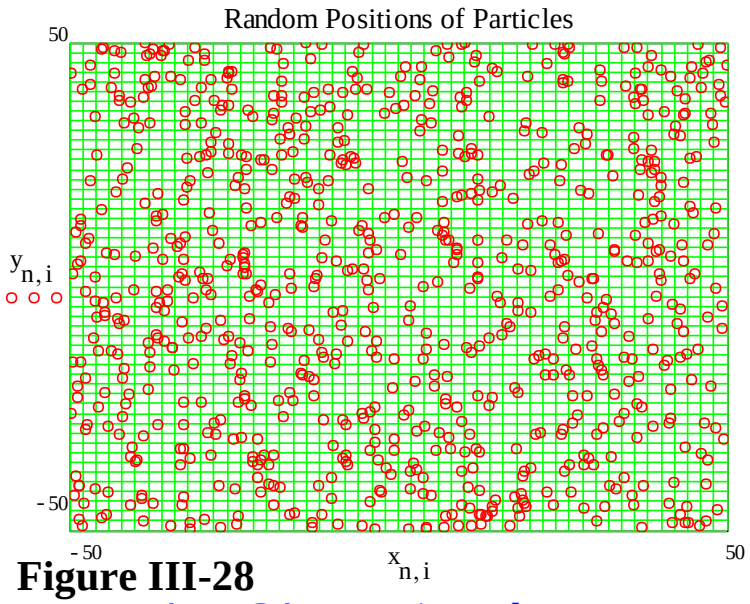

Figure III-28

MATHCAD_252\Random_Posit

per particle, where V is the volume of the gas container. Integration over the entire volume just cancels the term $1/V$ in this formula, ***the distribution is properly normalized***. It is illustrated in the two-dimensional figure, representing the positions of $N = 400$ particles in a box of 100×100 in units of the characteristic Lennard-Jones range parameter σ. This can be considered a snapshot of the particle positions at a given time. It represents, hence, a ***microstate of the system***. The random evolution in time of these positions is illustrated in an animation, illustrating the complex trajectory of this still relatively small system, as it passes from microstate to microstate.

Equ. III.125 gives an indication of the probability to find any of the particles of an ideal gas at a particular location $\vec{r}$. It contains no information about the ***relative positions or energies*** of two or more particles. For an ideal gas of non-interacting particles, it is natural to postulate that there are ***no spatial correlations*** between the particles

(***"molecular chaos"***). For real gases, however, where particles interact with each other, correlations and self-organization effects are expected. The particles are expected to cluster together, an interesting phenomenon of microscopic particles under active study, not only in physical chemistry, but in a number of different fields of science and for a large variety of different substances. In the limit of high densities and low temperatures, these effects lead to the formation of crystal lattices of high symmetries even for spherical particles, an effect that is not immediately obvious from the simple radial dependence of interaction forces.